applied sciences

MDPI

Article

Experimental Study on the Deformation and Mechanical Properties of Bamboo Forest Slopes

Hui Yang [1,2], Zhengyi Cao [2,*], Xueliang Jiang [1,2] and Yixian Wang [3]

[1] School of Civil Engineering and Engineering Management, Guangzhou Maritime University, Guangzhou 510725, China
[2] School of Civil Engineering, Central South University of Forestry and Technology, Changsha 410018, China
[3] School of Civil Engineering, Hefei University of Technology, Hefei 230009, China
* Correspondence: caozhengyi215@163.com; Tel.: +86-18940158267

Abstract: In this paper, model tests on a plain soil slope and a bamboo-rooted slope under slope top loading were carried out to analyze the slope surface displacement, the change in earth pressure, and the failure mode of the slope. Furthermore, the influence of rainfall on the deformation and mechanical properties of bamboo-rooted slope sliding was studied. The results show that: (1) the failure mode of the plain soil slope was block sliding failure, while the failure mode of the bamboo-rooted slope was progressive backward failure. (2) Under the slope top load, the slope displacement shows the rule that the top of the slope was large and the foot of the slope was small. The presence of bamboo rhizomes had a negligible effect on the slope displacement, but it significantly contributed to the sliding area's increase. (3) Compared with the plain soil slope, the earth pressure in the area of the foot of the slope under the same level of the load was elevated more obviously by the bamboo-rooted slope, which indicates that bamboo rhizomes could play a specific role in reinforcing the slope. Still, the scope of its influence was limited and mainly concentrated in the shallow soil. (4) There was a significant increase in the displacement of the bamboo-rooted slope under rainfall conditions, and the magnitude of the upward slope earth pressure was small in the process of step-by-step loading. The test results may have important guiding significance for the in-depth study of the instability law and disaster prevention in bamboo forest areas.

Keywords: bamboo rhizome; shallow landslide; rainfall infiltration; model test

Citation: Yang, H.; Cao, Z.; Jiang, X.; Wang, Y. Experimental Study on the Deformation and Mechanical Properties of Bamboo Forest Slopes. *Appl. Sci.* **2023**, *13*, 470. https://doi.org/10.3390/app13010470

Academic Editor: Cheng-Yu Ku

Received: 12 December 2022
Revised: 23 December 2022
Accepted: 26 December 2022
Published: 29 December 2022

1. Introduction

Landslide hazards frequently occur in forested mountains. Their triggering conditions are closely related to the type of vegetation and root–soil interaction on the mountains, in addition to factors such as topography, geomorphology, geological structure, landslide morphology, and rainfall [1–4]. The survey results of geological disasters in the Hunan Province of China show that [5], from the distribution of density (at/100 km^2) of landslide disaster points in various vegetation types, the highest distribution of landslide density is bamboo forest, fir forest, and pine forest. Therefore, it is important to study the instability laws of the slopes of bamboo forest areas for disaster prevention.

The stability of bamboo forest slopes is tightly related to the underground stems of bamboo. Bamboo rhizomes mostly grow in shallow soil, showing undulating extensions in the ground, forming a horizontal mesh canopy. [6] Individual bamboo root systems are difficult to precisely delineate from other bamboo root systems. This is distinct from other tree species with separate and vertically growing root morphologies. Currently, three primary methods are used to study landslides in the bamboo forest area: field surveys [7–9], numerical simulations [10–12], and model tests. Field surveys can well establish the relationship between landslide areas and influencing factors such as plant coverage, plant type, and rainfall intensity, but it does not capture the deformation and

internal stress variations of the slopes during the slide. Numerical simulations can tightly control the uniqueness of variables, but test results are generated under ideal conditions and do not accurately reflect the failure of slopes. Model tests have excellent intuition, can control single variables more accurately, simulate complex boundary conditions, and reflect landslides' intrinsic interaction under conditions that satisfy similar principles [13]. The study of model tests on slopes in bamboo forest areas by domestic and overseas scholars is still in its infancy, but model tests on slopes using different types of plants still have strong reference implications. R. Sonnenberg et al. [14] conducted an experimental model study of groundwater-level-induced slope instability in willow roots. They explored the effect of willow roots on slope stabilization and failure modes. Chen Jie et al. [15] compared the changes in the soil hydraulic properties of three different vegetated slopes under rainfall conditions. They analyzed the effect of separate plant roots on the soil penetration coefficient. A. Askarinejad et al. [16] carried out two sets of centrifuge model tests on vegetated slopes and bare slopes under rainfall conditions. The results show that the infiltration capacity of the vegetated slopes is higher than that of the non-vegetated slopes, and that slopes with well-developed root networks may experience more significant deformations prior to failure. Yao-Jun Liu et al. [17] revealed the variation pattern between soil shear strength depreciation and slope erosion, runoff coefficient, and soil slip rate by four groups of vegetated slope rainfall model tests. Song Heung-Hua et al. [18] studied the failure of three plant slopes under the same rainfall condition. They found that the plant's root morphology had a more significant effect on the stability of the slopes, and that their strengthening effect was ranked from highest to lowest by Bermuda grass, Chinese holly, and tall fescue.

Most of the above results focus on the influence of plants with strong reinforcement on slope stability and their modification of soil mechanical and hydraulic properties. However, bamboo forest slopes, which are prone to landslides, have yet to be explored in depth. This paper takes the bamboo forest slope as the research object and uses the model test method to explore the changes in soil deformation and mechanical properties of the overlying bamboo forest slope in the sliding process with or without rainfall, to provide test data and reference the basis for studying the instability law of forest landslides and disaster prevention.

2. Materials and Methods

2.1. Similarity Ratio Design

The theoretical foundation of model tests is similarity theory. To design a landslide model test, certain similarity conditions should be selected according to the actual soil conditions, which generally include geometric similarity, physical-mechanical similarity, and boundary condition similarity [19]. In general, landslides are more likely to occur on steeper mountains [7] and choosing a larger similarity ratio is conducive to accurately reflecting the sliding properties of the prototype slopes. Considering the boundary size effects of the model box and the slope model, a bamboo forest slope satisfying the test requirements was selected in Jinpen Mountain, Taojiang County, Yiyang City, Hunan Province, China. Finally, the similarity ratio of the slope model is determined to be 1:7, and the slope angle of the model is 45°. In order to simplify the test process and highlight the research subject of the test, the model slope was divided into two parts: an upper layer of clayey soil and a lower layer of bedrock. There is a section of platform at the top and foot of the slope. The test prototype slope is shown in Figure 1. The similarity of the physical quantities for each model test is shown in Table 1.

Figure 1. Jinpen Mountain bamboo forest.

Table 1. Similarity ratio of physical quantities in model tests.

Type	Physical Quantities	Dimension	Similarity Relation	Similarity Ratio
Material properties	Stress σ	FL^{-2}	$C_\sigma = C_E C_\varepsilon$	7
	Strain ε	—	$C_\varepsilon = {C_E}^{-1} C_l C_\rho$	1
	Elastic modulus E	$ML^{-1}T^2$	C_E	7
	Poisson's ratio μ	—	C_μ	1
	Density ρ	ML^{-3}	C_ρ	1
	Cohesion C	$ML^{-1}T^2$	$C_C = C_E C_\varepsilon$	7
	Internal friction angle φ	—	—	1
Geometric properties	Geometrical length L	L	C_l	7
	Displacement u	L	$C_u = C_l {C_\varepsilon}^{-1}$	7
Boundary Condition	Rainfall intensity q	LS^{-1}	$C_q = \sqrt{C_l}$	$\sqrt{7}$
	Time t	S	$C_t = \sqrt{C_l}$	$\sqrt{7}$

2.2. Test Material

The test soil was a clayey soil from the bamboo forest area of Jinpen Mountain. The retrieved clayey soil was passed through a 1 cm diameter sieve to filter out large stones. Sieved clayey soil was used to simulate the main part of the slope. A 50 cm thick layer of barite powder was used to simulate the bedrock at the base of the slope. A range of the physical and mechanical parameters of the soil were measured by conventional geotechnical tests. The particle analysis test shows that the uniformity coefficient Cu = 8.11, the curvature coefficient Cc = 1.68, and the gradation was good. The parameters of clay soil and barite powder for specific tests are shown in Table 2.

Table 2. Parameters of the soil.

Soil Type	Unit Weight/ (kN/m^3)	Maximum Dry Density /(g/cm^3)	Poisson's Ratio	Cohesion/ kPa	Internal Friction Angle/(°)	Optimum Water Content/(%)
Clay soil	18.37	1.85	0.32	12	18.5	14.5
Barite powder	21.58	1.94	0.38	18	22.5	—

The well-developed underground root system of bamboo consists of rhizomes and stumps. Bamboo stumps have bamboo poles at the top and bamboo rhizomes at the bottom. Bamboo rhizomes grow horizontally in the soil, forming a web-like structure that is an essential component of the bamboo roots. Typically, a bamboo forest is connected as a whole by its complex underground root system, so the main factor affecting slope stability is the leading underground part of the bamboo, the bamboo rhizomes. On the prototype slope of Jinpen Mountain, three areas of 1 m^2 were selected to be excavated to a depth of 25 cm. After removing the soil containing the bamboo rhizomes, the two were separated to obtain complete bamboo rhizomes. The mass ratio of root to dry soil was defined as root content [20], and the average root content in these three areas was calculated to be 0.53%. In the model tests, appropriate lengths and weights of bamboo rhizomes were selected and buried into the model slopes, where the root content was controlled to be around 0.53%. The morphology of the bamboo rhizomes is shown in Figure 2. The parameters of the bamboo rhizomes are shown in Table 3.

Figure 2. Morphology of the bamboo rhizomes.

Table 3. Parameters of the bamboo rhizome.

Material Name	Elastic Modulus/ (kPa)	Tensile Strength /(MPa)	Poisson's Ratio	Volume Weight/(kN/m^3)
Bamboo rhizome	322.3	23.06	0.28	7.8

2.3. Testing Device

The indoor model test setup included a model box, a slope top loading system, a rainfall simulation system, and a measurement system. The details are as follows.

(1) Model box. The L × W × H was 360 cm × 150 cm × 200 cm. Both sides of the model box were made of transparent acrylic plates. The interior was taped with yellow tape to outline the dimensional edges of the designed slope to facilitate subsequent filling and comparison of the displacement changes in the soil before and after the test. To miniaturize the boundary effect of the sidewalls of the model box on the soil, Vaseline was uniformly applied to the interior of the box walls before each slope filling.

(2) Slope top loading system. This system included a jack, a pull pressure sensor, a ball seat, a distribution beam, an iron plate, and a wedge block. To simulate the sliding process of the slope, wedge blocks were buried at the top of the slope to increase the sliding thrust transmitted to the outside of the slope by the jack above. The ball seat

placed under the sensor can keep the force of the jack vertically downward to the distribution beam, and then the distribution beam and iron plate would convert the force into a uniform load applied to the upper surface of the wedge block to achieve the loading of the slope top.

(3) Rainfall simulation system. This included angle steels, a water supply piping system, rainfall nozzles, and a flowmeter. The spraying diameter of each rainfall nozzle was 1 m, and the spraying flow rate was 0.8 L/h. There were eight nozzles in total, which were connected through the water supply pipeline. Two rainfall nozzles were fixed on each angle steel, and the angle steels were spaced 60 cm apart and evenly arranged above the model box. A flowmeter was connected to the delivery pipe and was able to measure the amount of liquid passing at a rate of 1–40 L/min. The rainfall system was able to simulate an effective rainfall area of 5 m^2, the rainfall intensity could be controlled at 0–20 mm/h, and the average rainfall uniformity was 82%.

(4) Measurement system. The data acquisition system included an IMC_CRFX_400 dynamic data collector and a DH3821 data collector. The displacement and earth pressure sensors adopted the YWD-100-type strain displacement sensor and DMTY-type earth pressure cell, respectively.

2.4. Test Program

There were three model tests: a plain soil slope, a bamboo-rooted slope, and a rainfall bamboo-rooted slope.

Test G1 was a plain soil slope. A total of nine earth pressure cells numbered S1–S9 were buried in the model slope, five of which were arranged along the direction parallel to the slope surface, 25 cm away from the slope surface, and 24 cm apart from each other. The other five measurement points were arranged at the bottom of the slope at a distance of 10 cm from the barite powder layer, with a distance of 28 cm between them. Two rows of measurement points shared the same earth pressure cell S5 at the foot of the slope. Five displacement measurement points were laid on the slope surface, from the top to the foot of the slope in the order of D1–D5. D5 was 5 cm away from the foot of the slope, and then a displacement measurement point was arranged at every 24 cm along the slope side up. To ensure that more effective data variations could be measured, all earth pressure cells and displacement meters were placed on the central axis of the model slope. The test G1–G3 sensor arrangement is shown in Figure 3.

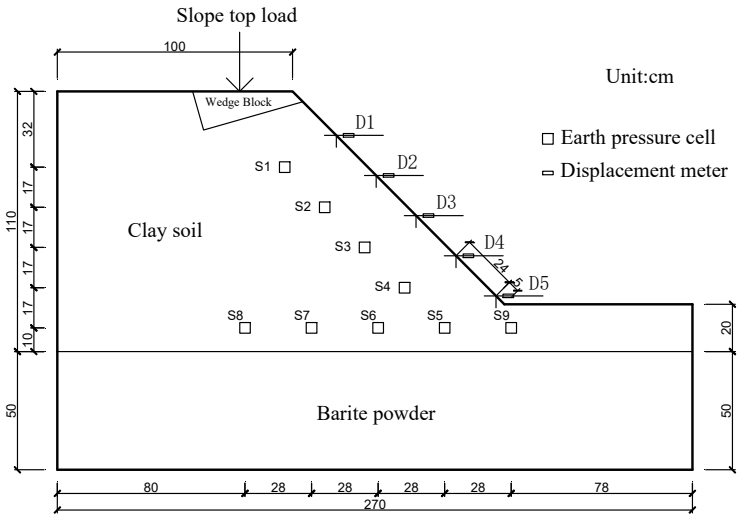

Figure 3. Test G1–G3 sensor arrangement.

Test G2 was a bamboo-rooted slope. According to the preset root content of 0.53%, six bamboo rhizomes of about 75 cm in length and six of about 40 cm in length were selected, stacked on top of each other, and buried parallel to the slope to a depth of 15 cm. The soil

was covered with bamboo rhizomes, and the slope was compacted and then chipped. The sensor arrangement in the model slope was the same as in test G1. The embedment of bamboo rhizomes is shown in Figure 4.

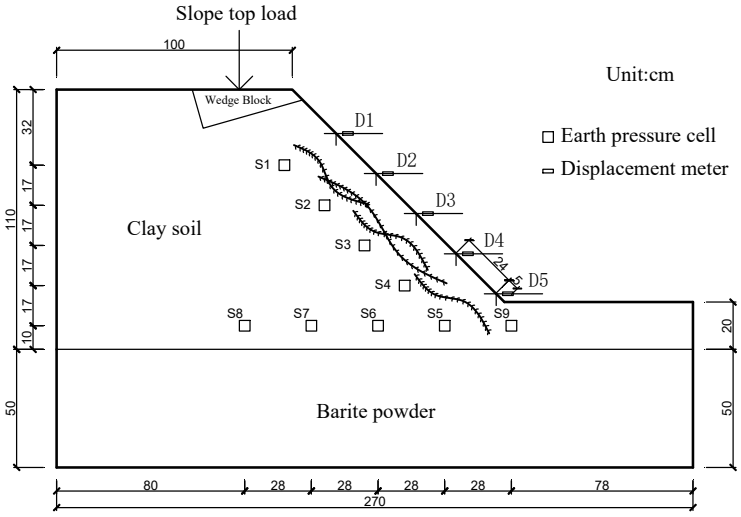

Figure 4. Schematic diagram of bamboo rhizomes' embedment.

Test G3 was a rainfall bamboo-rooted slope. A rainfall simulation system was used at the beginning of the test to apply rainfall conditions to the slope top, slope face, and slope toe locations. The rainfall intensity was 20 mm/h, and the duration was one hour. After rainfall, it was left for four hours to allow the water to penetrate completely before being loaded. This rainfall intensity and duration could ensure the infiltration of rainwater to the location of the soil layer where the bamboo rhizomes were located. The arrangement of sensors within the slope and the embedment of bamboo rhizomes were the same as in test G2. The rainfall simulation system is shown in Figure 5.

Figure 5. Rainfall simulation system.

All three model tests were filled in layers and compacted into 10 cm layers. The water content was controlled to be around 13%, and the compaction was near 80%. Graded loading on the top of the slope was observed, with each level of the load increasing by 5 kN. When the preset load was reached, the load was maintained for 1 min until the sensor readings were substantially stable. Then, the next level of loading was carried out until the model slope was significantly damaged. The slope should be left standing for more than a

week before the test to ensure that the bamboo rhizomes and the surrounding soil can be tightly integrated and to eliminate the settlement of the soil due to its gravity.

3. Results

3.1. Deformation Failure Characteristics Analysis

Figure 6 shows the failure of the slope after each group of test loading. In the initial stage of the slope top load applied to test G1, the soil deformation mainly occurred at the top position of the slope. With the load increase, the top of the slope produced a large settlement, and the soil was gradually compacted. The soil on the left edge of G1 started to slip from the foot of the slope area when 75 kN was applied, and then the soil on the right edge began to slip from the foot of the slope area when the load was 110 kN. The soil at the top of the slope gradually collapsed from both sides to the middle under the action of the higher load, and the soil in the middle sliding part continued to bulge in the direction of the outer side of the slope until the loading was complete. In test G2, the critical load at which sliding occurred was increased. Sliding occurred on the left and right edges of the soil when the slope was loaded to 85 kN and 90 kN in a similar form to G1, respectively, but the area where sliding occurred was increased. The multi-stage sliding failure occurred in the soil near the foot of the slope when it was loaded to 105 kN, followed by a slight local sliding failure in the lower right part of the side slope at 110 kN. The sliding body showed a trend of backward sliding failure. As can be seen from Figure 6c, the extent of slippage in the soil of test G3 was not as evident as in the first two sets of tests. In the process of increasing load, the soil did not show the phenomenon of the slipping of fine soil particles. However, it is noteworthy that when the top load of the slope was applied to 95 kN, the slider slid suddenly and formed a penetration crack from left to right in the middle and lower part of the slope and expanded rapidly with the increase in the load. In summary, under the action of the load on the top of the slope, block sliding failure occurred in test G1, and progressive backward failure occurred in test G2. After rainfall, test G3 soil slid without obvious signs and protruded in the direction of the outward slope as a whole.

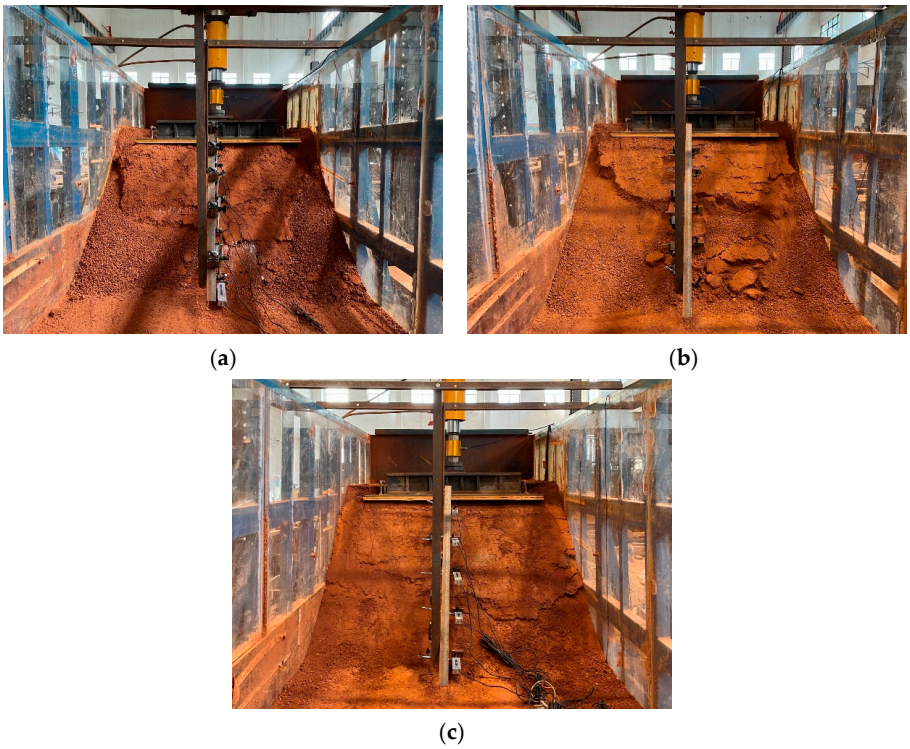

(**a**) (**b**)

(**c**)

Figure 6. Slope failure after loading in each group of tests. (**a**) Test G1 plain soil slope. (**b**) Test G2 bamboo-rooted slope. (**c**) Test G3 rainfall bamboo-rooted slope.

3.2. Slope Horizontal Displacement Analysis

Figure 7 shows the variation in the horizontal displacement of the slope with the load on the top of the slope. As seen in Figure 7a, the critical load in test G1 that made the displacement of the five measurement points start to alter significantly was 30 kN. With increasing load, the displacements at D1, D2, and D3 all significantly increased. The displacement increase rate at these three measurement points was significantly increased when the load was loaded to 60 kN, and the maximum displacement occurred at D3 for about 40 mm. Combined with the failure to the slope, it is not difficult to find that the sliding surface of this set of slopes was located between measurement points D3 and D4. The soil on either side of the sliding surface suffered from shear failure, which made the soil above the sliding surface more prone to slip. As a result, D4 and D5, which were closer to the foot of the slope, did not shift significantly during loading. As seen in Figure 7b, the critical load in test G2 that made the displacement of the five measurement points start to alter was 20 kN. With the increase in load, the displacement at the foot of the slope increased for all measurement points except D5. When loaded to 65 kN, there was a more significant growth in the rate of displacement increase at each measurement point. The maximum displacement occurred at D2 around 43 mm. As seen in Figure 7c, the critical load in test G3 that made the displacement of five measurement points start to shift was 15 kN, and the displacement of each measurement point showed a roughly linear increase in the process of step-by-step loading. When the load was increased to 60 kN, the growth rate of displacement at each measurement point was raised, and the maximum displacement occurred at D2 of about 57 mm. Compared with test G2, the maximum displacement increase was about 32%.

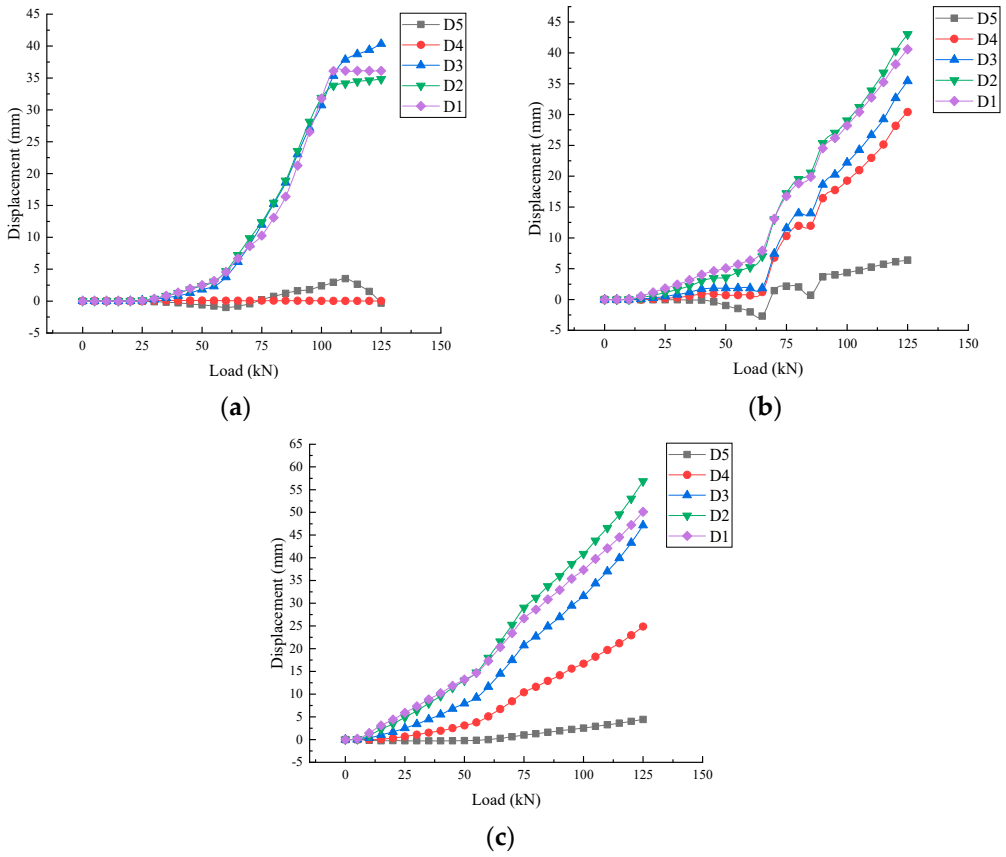

Figure 7. Variation of horizontal displacement in the slope with a slope top load. (**a**) Test G1 plain soil slope. (**b**) Test G2 bamboo-rooted slope. (**c**) Test G3 rainfall bamboo-rooted slope.

Figure 8a compares the displacement variation of measurement point D4 in each group of tests. Compared with test G1, the displacement increase in measurement point D4 in

test G2 was more apparent, and the sliding area of the slope increased significantly. This phenomenon was mainly caused by the intricate underground growth of bamboo rhizomes, with roots intertwining to form a web-like structure. Bamboo rhizomes drove additional soil to slide in the process of slope sliding

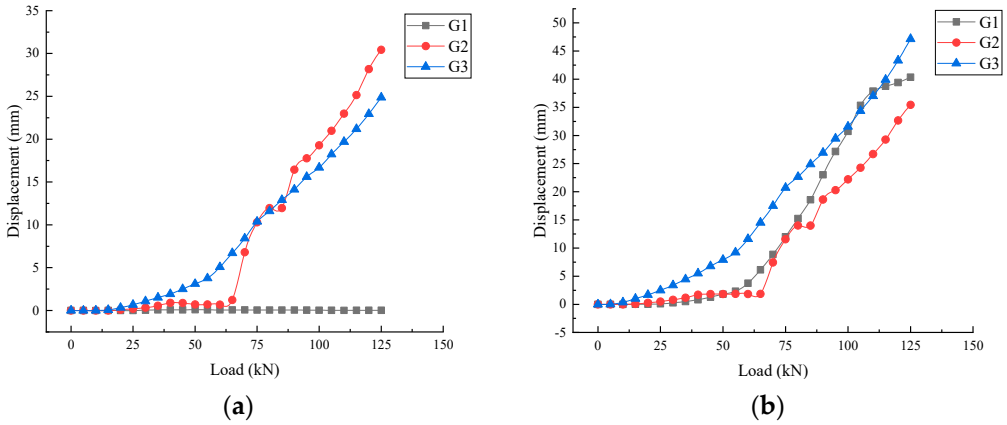

Figure 8. Displacement of representative measurement points in each group of tests. (**a**) Measurement point D4. (**b**) Measurement point D3.

Figure 8b compares the displacement variation of measurement point D3 in each group of tests. It can be found that the presence of bamboo rhizomes played a specific limiting role in the horizontal displacement of the slope and the stability of slope G2 was improved compared to slope G1. Due to the effect of rainfall, the displacements of measured point D3 on the slope of G3 were higher than those of G2 at all loading levels. This suggests that the stability of this slope was significantly reduced compared with that of slope G2

The above test results show that the slope displacement presented the rule that the top of the slope was large and the foot of the slope was little under the action of the load on the top of the slope. The addition of bamboo rhizomes had a slight effect on the maximum displacement of the slope, but it had a significant contribution to the increase in the sliding region. The displacement of the rainfall bamboo root slope showed an approximately linear increasing trend in the process of step-by-step loading. It produced the largest displacement among the three groups of slopes, which was less stable.

3.3. Slope Earth Pressure Analysis

The conventional method of laying out an earth pressure cell requires the support surface of the sensor to be fixed, with the force surface facing the direction of the force to be measured in the test. However, since the soil in this test slides, fixing the earth pressure cell will inevitably obstruct the soil's displacement. Therefore, only a simple transducer placement was made in the process. Based on this arrangement, the earth pressure will increase when the soil is compacted under the top load of the slope. If the soil slide causes the soil near the sensor to become less compact, the earth pressure is reduced.

3.3.1. Horizontal Earth Pressure Analysis along the Slope Direction

Figure 9 shows the variation of horizontal earth pressure with the slope top load at measured points along the slope direction. It can be seen from Figure 9a that in the initial loading stage of test G1, the earth pressure response at the measuring points S1 and S2, which were closest to the loading position, was more rapid and the amplitude increased more evidently. However, with the increase in load, S1 dropped at 95 kN and then continued to rise. This means that the soil near the measurement point had reached a new equilibrium state after the failure occurred under this load level, and the earth pressure rose again. The same unloading trend also occurred at measurement points S2 and S3. By analyzing the test data of these three measurement points, it was found that the soil above measurement point S3 was damaged during loading at the top of the slope. The

sliding surface of the slope was between measurement points S3 and S4, corresponding to a shift of the slope G1. Compared with test G1, the number of measurement points where unloading occurred in test G2 was significantly reduced. Only a minor amount of unloading occurred at measurement point S2, which was closer to the loading area at the top of the slope. During the initial loading process, there was no obvious pattern in the magnitude of earth pressure shift at each measurement point along the slope in the direction of test G1. However, in test G2, the earth pressure of S1 and S2, which were close to the loading position of the slope top, was invariably smaller than that of S3 and S4, which were located in the middle of the slope. This suggests that bamboo rhizomes may be more effective in limiting the deformation of the soil located in the lower and middle parts of the slope, resulting in less displacement and higher earth pressure under the same load. Under rainfall conditions, the soil capacity of the slope increased due to the infiltration of rainwater, which created a substantial initial earth pressure at the beginning of loading. The rainfall boundary was applied at the slope's top, surface, and foot, so rainwater infiltration was more at the top and less at the foot of the slope. Therefore, the initial earth pressure of measurement points S1 and S2, located at the top of the slope, was larger than that of other measurement points. The incremental magnitude of earth pressure at each measurement point during step-by-step loading was considerably smaller than in the first two sets of tests. This shows that due to the infiltration of rainwater, the effective stress between soil particles and particles decreased, and the slope had a greater displacement under the same load, which reduced the compactness of the soil at each measuring point significantly. The absence of a stable support surface for the earth pressure cell resulted in a significant reduction of the earth pressure in this set of working conditions compared to slope G2.

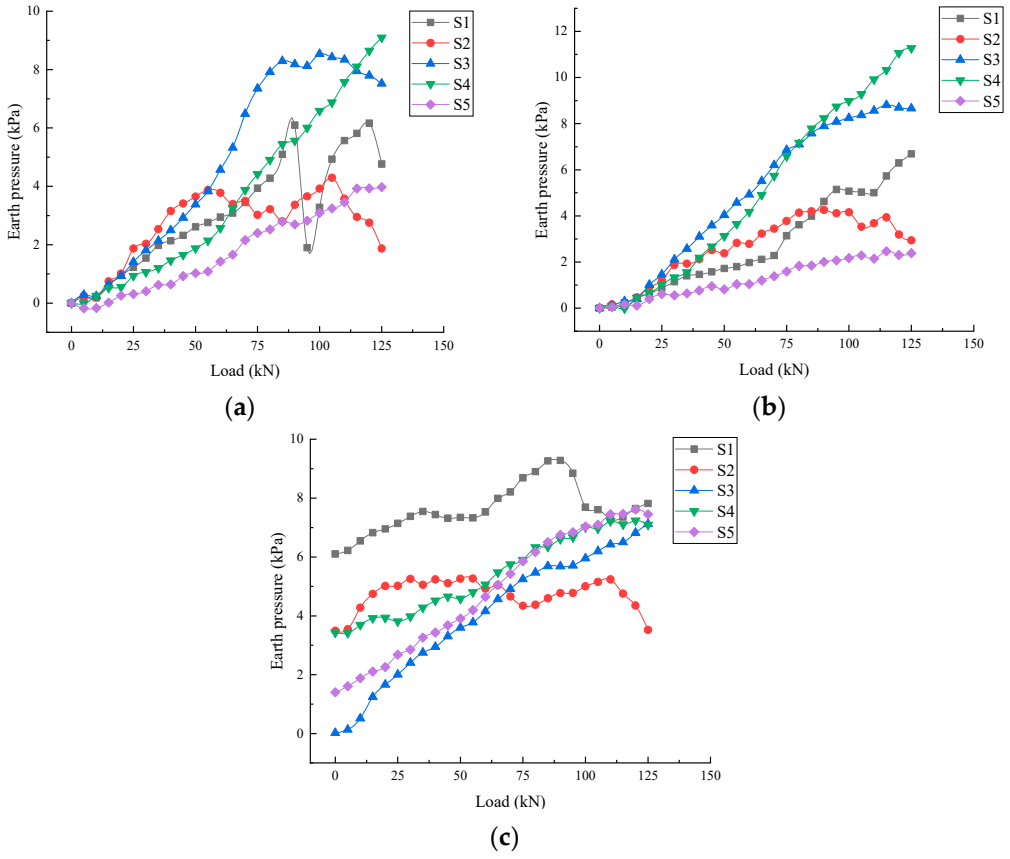

Figure 9. Variation of horizontal earth pressure at measured points along the slope with the slope top load (**a**) Test G1 plain soil slope. (**b**) Test G2 bamboo-rooted slope. (**c**) Test G3 rainfall bamboo-rooted slope.

Figure 10a compares the variation of earth pressure measurement point S2 with the slope top load in each group of tests. Since the measurement point S2 was close to the location of the top load, the earth pressure at this measurement point in each group of tests produced different degrees of unloading phenomenon during the step-by-step loading process. Through comparison, it can be found that the soil of slope G3 in the three groups of tests could not continue to bear higher loads at first, and the earth pressure at the measuring point S2 did not evidently increase, only when loaded to 20 kN. The second was slope G1; the unloading load level was 55 kN. The highest load level that can be supported was slope G2, and the load level for unloading was 90 kN. Under rainfall conditions, there was a significant decrease in the amplitude of earth pressure at measurement point S2 with the rise in load. The variation amplitude of earth pressure at measuring point S2 in test G3 was 1.78 kPa, which was 58% lower than that of 4.26 kPa in test G2. Observing the shift in displacement measurement point D2 near test earth pressure measurement point S2 in both groups, it was found that the maximum displacement of test G3 at D2 was 56.85 mm, which was improved by about 32% compared with the maximum displacement of test G2 at D2 of 43.03 mm. This further indicates that the soil deformation released the earth pressure inside the slope, and the two data can be corroborated with each other.

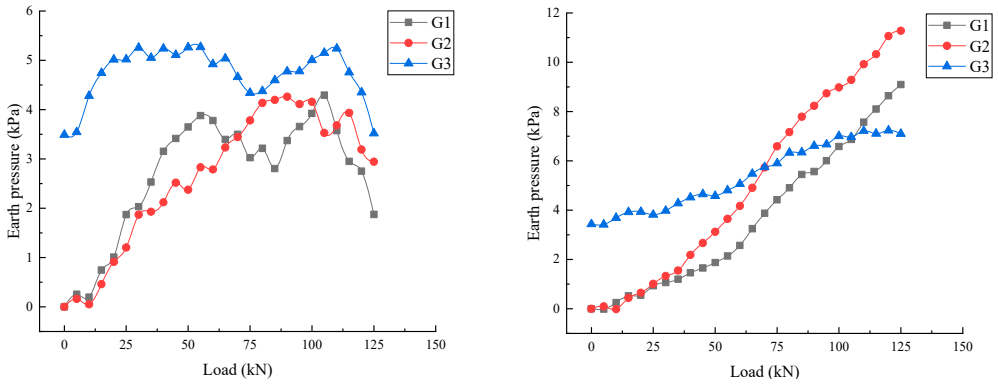

Figure 10. Earth pressure of representative measurement points in each group of tests. (**a**) Measurement point S2. (**b**) Measurement point S4.

Figure 10b compares the variation of earth pressure measurement point S4 with the slope top load in each group of tests. It can be seen that the earth pressure at measurement point S4 in test G2 was greater than that in test G1 under all levels of loading. The maximum earth pressure at measurement point S4 in test G2 was 11.28 kPa, which was approximately 24% higher than the maximum earth pressure of 9.1 kPa at measurement point S4 in test G1 under the same level of loading. In contrast, the value-added earth pressure at measurement point S4 in test G3 was only 3.81 kPa, which was only 34% of the same measurement point in G2. This suggests that the bamboo rhizomes had a favorable reinforcement effect at the location near the foot of the slope. Still, the reinforcement effect of the bamboo rhizomes was fragile under the rainfall condition and could not limit the deformation of the soil. The above test results suggest that the bamboo rhizomes could play a specific restraining effect on the rear soil. They could increase the bearing capacity of the soil, reduce the occurrence of unloading, and improve the earth pressure at the foot of the slope under the same load. Rainfall significantly reduced the stability of the slope, and the earth pressure uplift value was inferior in the process of increasing load at the top of the slope. This indicates that the soil was uncompacted during the loading process and was more prone to landslides.

3.3.2. Horizontal Earth Pressure Analysis along the Bottom of the Slope

Figure 11 shows the variation of horizontal earth pressure with the slope top load at the measured points along the bottom direction of the slope. From Figure 11a, it can be seen that the slope of earth pressure rise at S7 started to exceed the remaining four

measurement points significantly when the load was applied to 30 kN, and the horizontal soil pressure at this point reached 10.97 kPa when the load was applied to 125 kN. This is mainly because the top of the slope is loaded with a wedge block. During the step-by-step loading process, the most direct-action area of the load at the bottom of the slope was located near the measuring point S7. The same pattern was present in the data of test G2 and test G3. As seen in Figure 11b, there was a tendency for the earth pressure in the direction of the bottom of the slope under the top load of test G2 to gradually decay from the center of measurement point S7 to both sides. Under the higher-level load, the earth pressure at each measurement point was S7, S6, S8, S5, and S9 from high to low. The difference in earth pressure at each measurement point was prominent, while the earth pressure at measurement points S5, S6, and S8 in test G1 was similar in magnitude. This indicates that the existence of bamboo rhizomes limited the displacement of the soil at the bottom of the slope, and there was an essential condition for the increase in earth pressure during the step-by-step loading process. As seen in Figure 11c, there was initial earth pressure at each measuring point at the beginning of the test due to the rainfall in test G3. Still, since the measurement points were located at the bottom of the slope, they were less affected by the rain than the measurements along the slope surface direction. The earth pressure at measurement points S5, S6, and S8 in this group of tests had a similar trend of shift during the process of step-by-step loading, and the phenomenon of the gradual decay of load from S7 to both sides in the direction of the slope bottom was not evident.

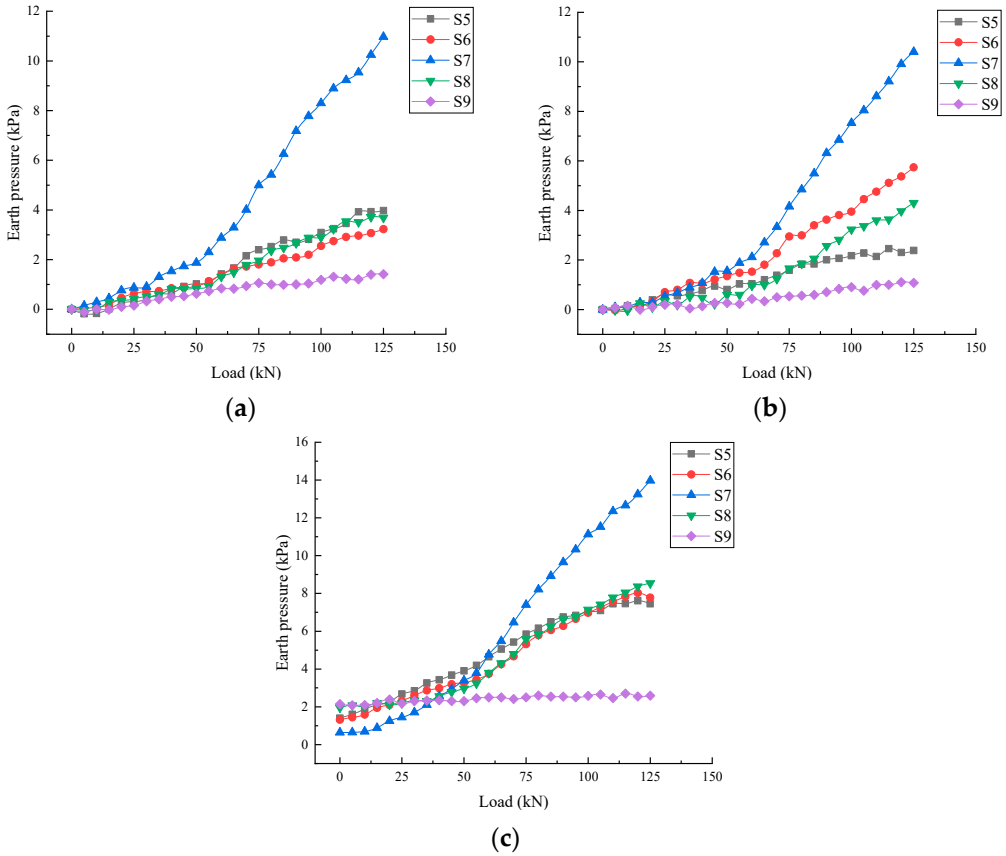

Figure 11. Variation of horizontal earth pressure at measured points along the bottom of the slope with the slope top load (**a**) Test G1 plain soil slope. (**b**) Test G2 bamboo-rooted slope. (**c**) Test G3 rainfall bamboo-rooted slope.

Figure 12a compares the variation of earth pressure measurement point S6 with the slope top load in each group of tests. When the load was less than 65 kN, the magnitude of earth pressure at measurement point S6 was relatively consistent in tests G1 and G2. In contrast, when the load exceeded 65 kN, it was evident that the earth pressure at

measurement point S6 in test G2 had a relatively significant increase. This suggests that the bamboo rhizomes could also play a relatively good role in enhancing the slope in the bottom direction of the slope under high-grade loads. The trend of earth pressure change with the slope top load at measurement point S6 in test G3 was roughly the same as in test G2, indicating that the influence of rainfall boundary on earth pressure at this measurement point was dominated by changes in the initial earth pressure.

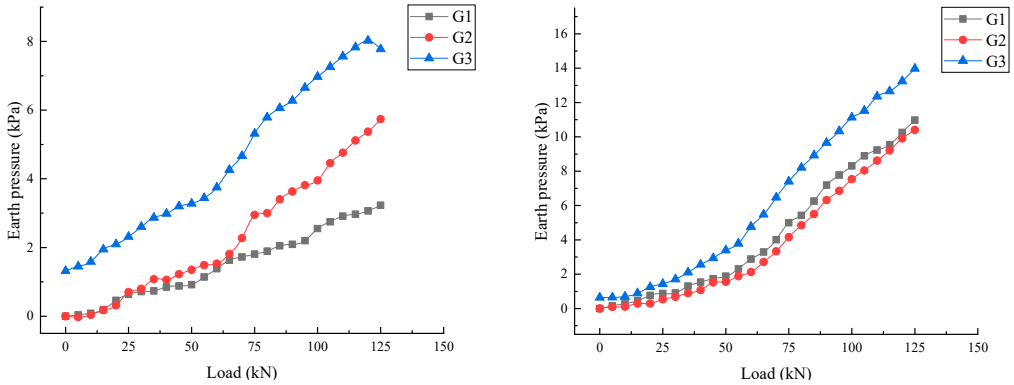

Figure 12. Earth pressure at representative measurement points in each group of tests. (**a**) Measurement point S6. (**b**) Measurement point S7.

Figure 12b compares the variation of earth pressure measurement point S7 with the slope top load in each group of tests. Comparing the data, it can be seen that the magnitude of earth pressure at measurement point S7 was generally consistent with the load increase in tests G1 and G2, indicating that the bamboo rhizomes had a negligible effect on the earth pressure at measurement point S7. Combined with the location of the measurement points in the slope, it can be found that the influence of the bamboo rhizomes on the back soil ranged between measurement points S6 and S7.

The above test results show that the horizontal earth pressure in the bottom direction of the slope decreased from the center of the measuring point S7 to both sides under the top load of the slope. The bamboo rhizomes strongly influenced the stability of the shallow soil, and the measurement points closer to the bamboo rhizomes had higher earth pressure under the same load level. The influence of rainfall on the horizontal earth pressure of the soil at the bottom of the slope was mainly concentrated in part nearer to the slope, while the effect on the horizontal earth pressure of the soil deep inside the slope was minor.

4. Discussion

The above study analyzed the effects of single variables of bamboo rhizomes and rainfall on the deformation and mechanical properties present during the sliding of slopes. However, the impact on the soil in the case of mutual coupling between the two still requires additional exploration. The coupling effect can be reflected in the superposition of the values of a certain characteristic of the slope. Therefore, it is valid to compare the displacement and earth pressure in test G3 with that in test G1 to derive the coupling effect of bamboo rhizomes and rainfall. Then, ensuring that the bamboo rhizomes and rainwater are in a coupled state is a prerequisite for the test results to be usable and relevant. At the end of test G3, soil samples at the depths of 5 cm, 10 cm, 15 cm, 20 cm, and 25 cm were selected from three measuring points at the slope's lower, middle, and upper parts, and the samples were tested for water content. The distribution of measurement points is shown in Figure 13. The water content at different depths of each measurement point is shown in Table 4.

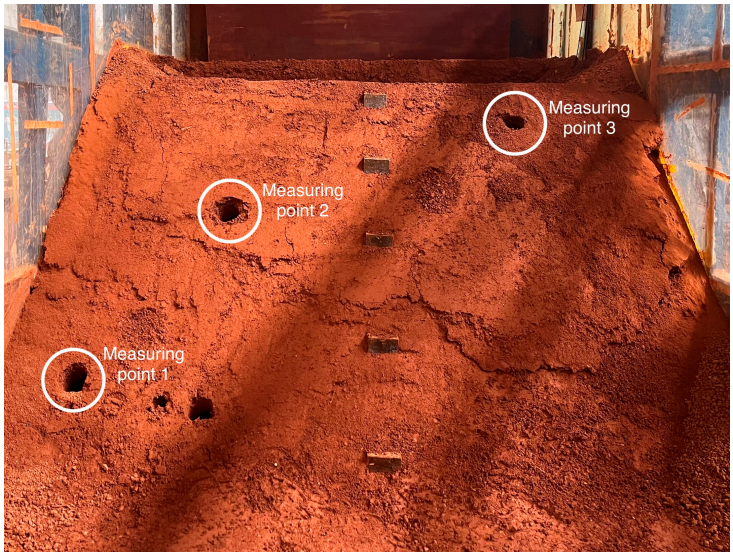

Figure 13. Distribution of water content measuring points.

Table 4. Water content at different depths of each measuring point.

Water Content ω	Depth of Soil Layer				
	5 cm	10 cm	15 cm	20 cm	25 cm
Measuring point 1	26.05%	24.16%	27.13%	16.70%	13.35%
Measuring point 2	23.14%	24.14%	24.52%	23.13%	17.81%
Measuring point 3	21.95%	22.87%	24.88%	23.88%	23.50%

Combined with the water content of the soil at the beginning of the test (about 13%), the water content of the soil increased significantly at a depth of 15 cm with bamboo rhizomes. This indicates that during the infiltration of rainfall; the infiltration peak had reached and passed where the bamboo rhizomes were situated. Therefore, the results of test G3 were produced with coupled bamboo rhizomes and rainfall

In Figure 8b, the displacement of measuring point D3 in test G3 is the result of the interaction between the restraining effect of bamboo rhizomes on soil and the weakening effect of rainfall on soil. At the initial loading stage, the displacement of slope G3 at measurement point D3 increased faster with the load. When the load reached 60 kN, the displacement growth rate of measurement point D3 in slope G1 exceeded that of slope G3. During the subsequent loading process, the deformation of slope G1 increased significantly. When the load at the top of the slope was close to 100 kN, the displacements of the two groups of slopes at this point were already relatively close. The above test results show that the weakening effect of rainfall on the soil body accounts for the main effect when the slope does not produce large deformation. After the slope was deformed, the restraining effect of the bamboo rhizomes gradually appeared, and it was more evident at the middle and lower positions of the slope. However, it is worth noting that the displacement of slope G3 exceeded that of slope G1 under higher load, which indicates that the restraining ability of bamboo rhizomes to soil is limited. Comparing the variation of soil pressure in the vicinity of this displacement measurement point, under the action of the top load, the soil pressure rise of slope G3 was smaller than that of slope G1, which also confirmed the displacement variation.

Moreover, by comparing with the previous studies, the test results of this experiment also have the following similarities and differences. The sliding area of slope G2 in the test increased compared to slope G1, which is more similar to the test results of A. Askarinejad et al. [16] Namely, slopes with well-developed root networks may experience greater deformation before failure, while the interconnected root network may mobilize a

larger volume of unstable soil during the failure process. The bamboo rhizomes used in this experiment have more complex fibrous roots and thicker underground stems than the Avena Sativa (from the family of oats) seeds used in A. Askarinejad's study. Therefore, the phenomenon of increasing the area of sliding in the bamboo root slope is more obvious and mainly occurs in shallow soil.

It is noteworthy that block sliding failure of slope G1 and progressive backward failure of slope G2 were observed in this paper. In contrast, R. Sonnenberg et al. [14] found that the failure mode of fallow slopes was progressive blockwise failure, and the failure mode of planted slopes was block sliding failure. The reason for the different results may be related to the root morphology of the vegetation. The root morphology of bamboo rhizomes is intertwined and grows parallel to the slope, while a single willow plant has independent roots and grows vertically. In the slope's sliding process, the already deformed bamboo rhizomes below will drive the soil above to slide down, and then the progressive backward failure will occur.

5. Conclusions

Through three groups of indoor model tests, the soil deformation and mechanical properties present during slope sliding were studied. The following aspects can be obtained:

(1) The bamboo rhizomes could change the failure mode of the slope and make the slope change from block sliding failure to progressive backward failure. Their intertwined root system forms a net-like structure, which will drive more surface soil to slide down during the sliding process of the slope.
(2) In the process of applying the slope top load step-by-step, the horizontal displacement of the slope shows a trend that the top of the slope was large and the foot of the slope was small. Compared with the plain soil slope, the sliding area of the bamboo-rooted slope was significantly increased. Under rainfall conditions, the displacement of the bamboo root slope increased significantly. With the large deformation, the restraint effect of bamboo rhizomes on the soil gradually appeared. The displacement of each measuring point increased nearly linearly with the increase in slope top load.
(3) The bamboo rhizomes could better limit the deformation of the soil at the foot of the slope and improve the compactness of the soil behind the root. The increase in soil pressure at the foot of the slope was larger under the top load of the slope. However, the influence range of bamboo rhizomes on soil was limited, mainly concentrated in the area within 40 cm near the roots. Beyond this area, the reinforcement effect of bamboo rhizomes on soil was not obvious.
(4) Rainfall had a greater impact on the soil in the area closer to the slope surface, and the infiltration of rainwater reduced the effective stress between the soil particles. In the process of loading step-by-step, the slope deformed more, the soil was uncompacted, and the rise in earth pressure was smaller with the increase in load.

Author Contributions: Investigation, data curation, formal analysis, writing—original draft preparation, and writing—review and editing, Z.C.; supervision and validation, H.Y.; conceptualization and funding acquisition, X.J.; resources, Y.W. All authors have read and agreed to the published version of the manuscript.

Funding: This study was supported by the National Natural Science Foundation of China (31971727), the Science and Technology Innovation Program of Hunan Province (Grant No.: 2022NK2056), the Forest Science and Technology Innovation Program of Hunan Province (XLK202105-3), the Special Fund Project of Safety Production Prevention and Emergency Response of Hunan Province in 2021 (Grant No.: 2021-QYC-10008-24956), the Hunan Provincial Natural Science Foundation Project (Grant No.: 2022JJ31005), and the Key Construction Subject Scientific Research Ability Promotion Project of Guangdong Province (Grant No.: 2022ZDJS092).

Institutional Review Board Statement: Not applicable.

Informed Consent Statement: Not applicable.

Data Availability Statement: The original contributions presented in the study are included in the article. Further inquiries can be directed to the corresponding author.

Acknowledgments: The authors thank all those who provided assistance with this study.

Conflicts of Interest: The authors declare no conflict of interest.

References

1. Wang, X.; Ma, C.; Wang, Y.; Wang, Y.; Li, T.; Dai, Z.; Li, M. Effect of root architecture on rainfall threshold for slope stability: Variabilities in saturated hydraulic conductivity and strength of root-soil composite. *Landslides* **2020**, *17*, 1965–1977. [CrossRef]
2. Ghestem, M.; Veylon, G.; Bernard, A.; Vanel, Q.; Stokes, A. Influence of plant root system morphology and architectural traits on soil shear resistance. *Plant Soil* **2014**, *377*, 43–61. [CrossRef]
3. Hao, M.; Zhang, J.; Meng, M.; Chen, H.Y.H.; Guo, X.; Liu, S.; Ye, L. Impacts of changes in vegetation on saturated hydraulic conductivity of soil in subtropical forests. *Sci. Rep.* **2019**, *9*, 8372. [CrossRef] [PubMed]
4. Mehtab, A.; Jiang, Y.-J.; Su, L.-J.; Shamsher, S.; Li, J.-J.; Mahfuzur, R. Scaling the Roots Mechanical Reinforcement in Plantation of *Cunninghamia* R. Br in Southwest China. *Forests* **2021**, *12*, 33. [CrossRef]
5. Zeng, L.K.; Xu, M.; Fang, Q.; Li, J. Vegetation and development of geological hazards. *J. Geol. Hazards Environ. Preserv.* **2010**, *21*, 97–100.
6. China's Forests Committee. *China Forests. Vol. 4, Bamboo Forests, Shrublands, Economic Forests*, 2nd ed.; China Forestry Publishing House: Beijing, China, 2002; pp. 1845–1917.
7. Stokes, A.; Lucas, A.; Jouneau, L. Plant biomechanical strategies in response to frequent disturbance: Uprooting of *Phyllostachys nidularia* (Poaceae) growing on landslide-prone slopes in Sichuan, China. *Am. J. Bot.* **2007**, *94*, 1129–1136. [CrossRef] [PubMed]
8. Gong, Q.; Wang, J.; Zhou, P.; Guo, M. A Regional Landslide Stability Analysis Method under the Combined Impact of Rainfall and Vegetation Roots in South China. *Adv. Civ. Eng.* **2021**, *2021*, 5512281. [CrossRef]
9. Qin, M.; Cui, P.; Jiang, Y.; Guo, J.; Zhang, G.; Ramzan, M. Occurrence of shallow landslides triggered by increased hydraulic conductivity due to tree roots. *Landslides* **2022**, *19*, 2593–2604. [CrossRef]
10. Lin, D.-G.; Huang, B.-S.; Lin, S.-H. 3-D numerical investigations into the shear strength of the soil–root system of Makino bamboo and its effect on slope stability. *Ecol. Eng.* **2010**, *36*, 992–1006. [CrossRef]
11. Liang, T.; Knappett, J.A.; Duckett, N. Modelling the seismic performance of rooted slopes from individual root–soil interaction to global slope behaviour. *Géotechnique* **2015**, *65*, 995–1009. [CrossRef]
12. Świtała, B.M.; Wu, W. Numerical modelling of rainfall-induced instability of vegetated slopes. *Géotechnique* **2018**, *68*, 481–491. [CrossRef]
13. Zuo, Z.B.; Zhang, L.L.; Wang, J.H. Model tests on rainfall-induced colluvium landslides: Effects of particle-size distribution. *Chin. J. Geotech. Eng.* **2015**, *37*, 1319–1327.
14. Sonnenberg, R.; Bransby, M.F.; Hallett, P.D.; Bengough, A.G.; Mickovski, S.; Davies, M.C. Centrifuge modelling of soil slopes reinforced with vegetation. *Can. Geotech. J.* **2010**, *47*, 1415–1430. [CrossRef]
15. Chen, J.; Lei, X.-W.; Zhang, H.-L.; Lin, Z.; Wang, H.; Hu, W. Laboratory model test study of the hydrological effect on granite residual soil slopes considering different vegetation types. *Sci. Rep.* **2021**, *11*, 14668. [CrossRef] [PubMed]
16. Askarinejad, A.; Springman, S.M. Centrifuge modelling of the effects of vegetation on the response of a silty sand slope subjected to rainfall. In Proceedings of the Computer Methods and Recent Advances in Geomechanics: Proceedings of the 14th International Conference of International Association for Computer Methods and Recent Advances in Geomechanics, 2014 (IACMAG 2014), Kyoto, Japan, 22–25 September 2014; Taylor & Francis Books Ltd.: New York, NY, USA, 2015; pp. 1339–1344.
17. Liu, Y.-J.; Wang, T.-W.; Cai, C.-F.; Li, Z.-X.; Cheng, D.-B. Effects of vegetation on runoff generation, sediment yield and soil shear strength on road-side slopes under a simulation rainfall test in the Three Gorges Reservoir Area, China. *Sci. Total. Environ.* **2014**, *485–486*, 93–102. [CrossRef] [PubMed]
18. Song, X.H.; Tan, Y.; Zhang, S.J. Investigation on effects of vegetations on stability of sandy slope by indoor rainfall model test. *J. Harbin Inst. Technol.* **2021**, *53*, 123–133.
19. Yang, Z.J.; Cai, H.; Lei, X.Q.; Wang, L.Y.; Ding, P.P.; Qiao, J.P. Experiment on hydro-mechanical behavior of unsaturated gravelly soil slope. *Rock Soil Mech.* **2019**, *40*, 1869–1880.
20. Tongfa, D. *Stability Analysis Method of Vegetation-Slope System*, 1st ed.; China Architecture & Building Press: Beijing, China, 2016; pp. 15–22.